Journal of Rock Mechanics and Geotechnical Engineering 10 (2018) 669–677

Contents lists available at ScienceDirect

Journal of Rock Mechanics and Geotechnical Engineering

journal homepage: www.rockgeotech.org

Full Length Article

Compaction-induced stress in geosynthetic-reinforced granular base course – A discrete element model

Te Pei, Xiaoming Yang*

School of Civil and Environmental Engineering, Oklahoma State University, Stillwater, USA

ARTICLE INFO

Article history:
Received 7 August 2017
Received in revised form
29 January 2018
Accepted 31 January 2018
Available online 14 May 2018

Keywords:
Compaction
Geosynthetics
Granular soils
Numerical analysis

ABSTRACT

A discrete element method (DEM) model was used to simulate the development of compaction-induced stress in a granular base course, with and without geogrid reinforcement. The granular base course was modeled as a mixture of uniformly sized triangular particles. The geogrid was modeled as a series of equally spaced balls that interact with each other through long-range interaction contacts. The long-range interaction contact was also used to simulate a deformable subgrade. The compactor was modeled as a solid cylinder rolling at a constant speed. The DEM model shows that the geogrid-reinforced granular base course gains additional compaction-induced stress due to the residual tensile stress developed in the geogrid. The residual tensile stress in the geogrid increases with the number of compaction passes. Parametric analyses were also conducted to assess the effects of geogrid stiffness and subgrade modulus on the compaction-induced stress.

1. Introduction

Compaction is an important earthwork procedure during the construction of civil engineering structures such as pavements, embankments, retaining walls, and foundations. The compaction of granular soils is usually achieved by a few passes of a roller compactor until the desired dry density is reached. It is well known that compacted granular soils exhibit improved engineering properties such as increased stiffness and shear strength, and reduced permeability. In addition to the improved engineering properties, compaction also produces an increased lateral earth pressure in granular soils compared to the lateral earth pressure at rest. The increased lateral earth pressure is often referred to as the compaction-induced stress or the "locked-in" stress (Duncan and Seed, 1986; Seed and Duncan, 1986). The compaction-induced stress helps compacted soils gain additional strength and stiffness due to the stress-dependency of granular materials.

The development of compaction-induced stress is particularly important for roadway pavements with a granular base course, because the stiffness of the base course significantly affects the performance of the pavement structure. When a granular soil is reinforced by geosynthetic products such as geogrids, it usually suggests that a larger compaction-induced stress will be developed in the reinforced soil due to the interlocking effect between the geogrid and the soil. This phenomenon may have contributed to the increased stiffness of geosynthetic-reinforced granular base in the early stage. Although limited experimental data are available, partially due to the technical difficulty in the lateral earth pressure measurement in granular soils, a small number of published researches have supported the above hypothesis. For example, Kwon and Tutumluer (2009) compared dynamic cone penetrometer (DCP) test results in an unreinforced base course and a geosynthetic-reinforced base course and found that the reinforced base course showed a higher as-built stiffness. Another field study of intelligent compaction (Chang et al., 2011) also showed that the geogrid-reinforced base course showed an overall higher and more uniform stiffness than the control case after the same number of compaction passes.

The as-built stiffness of the granular base course is an important parameter in the roadway pavement design. Ideally, the increased stiffness of the reinforced base course layer due to the compaction-induced stress should be estimated and reflected in the pavement design. In the past, several design models (Perkins, 2001; Kwon et al., 2009; Wu and Pham, 2010; Yang et al., 2013) have been proposed to predict the compaction-induced stress in the design of reinforced flexible pavements. For example, Perkins (2001) suggested a residual tensile strain of 1% in the geosynthetic due to the effect of construction. Yang et al. (2013) proposed to modify the Duncan and Seed

* Corresponding author.
E-mail address: geoyxm@gmail.com (X. Yang).
Peer review under responsibility of Institute of Rock and Soil Mechanics, Chinese Academy of Sciences.

https://doi.org/10.1016/j.jrmge.2018.02.005

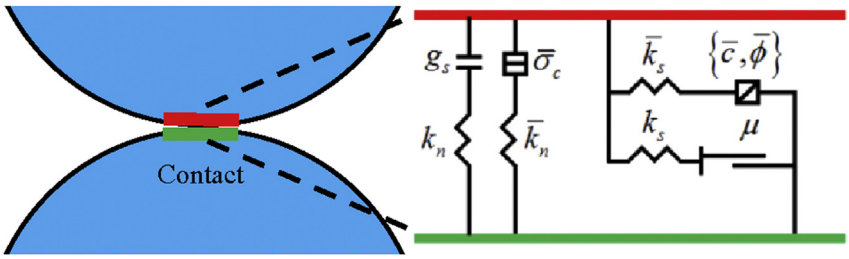

(a) Linear parallel bond model.

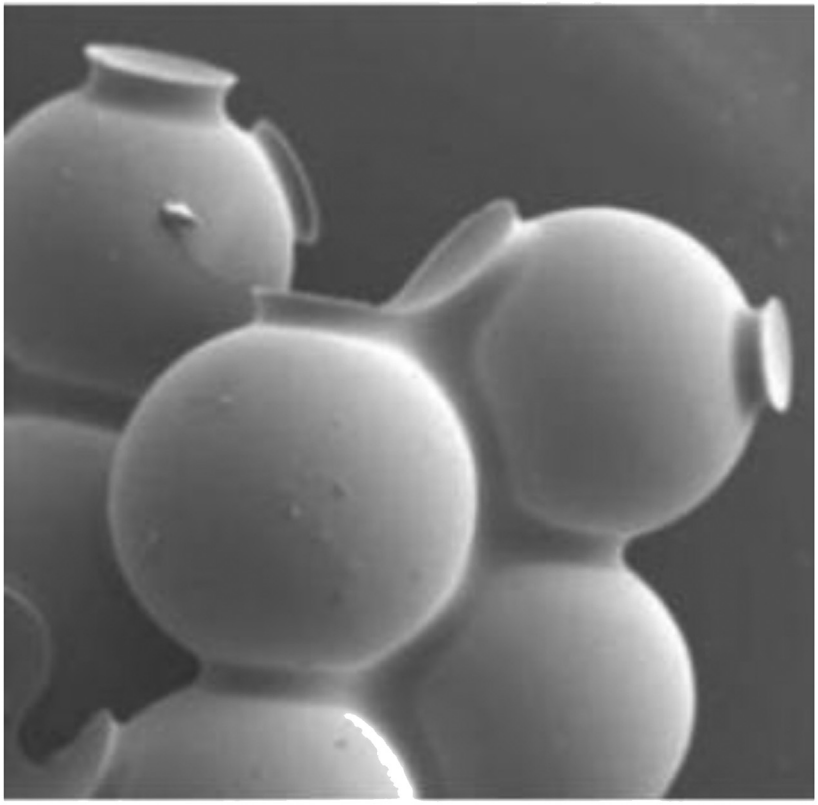

(b) Example of glass beads cemented with epoxy.

Fig. 1. Linear parallel bond model (Itasca, 2017) and an example.

(1986) model to consider the confinement effect of geosynthetics. However, none of the previous studies has well established the relationship between the compaction-induced stress and the material properties of geosynthetic, granular soil and subgrade.

This paper presents a two-dimensional (2D) discrete element method (DEM) model for the compaction process on a granular base course layer underlain by a deformable subgrade. The objective of the study is to build a numerical simulation tool to qualitatively investigate the phenomenon of compaction-induced stress in a layer of coarse-grained soil with and without geogrid reinforcement. The DEM model was developed with the computer program PFC™ 5.0 developed by Itasca (2017).

Table 1
Linear parallel bond model parameters.

Material	Linear group			Parallel-bond group					
	Friction coefficient, *fric*	Effective modulus, *emod* (MPa)	Normal-to-shear stiffness ratio, *kratio*	Tensile strength, *pb_ten* (MPa)	Cohesion, *pb_coh* (MPa)	Friction angle, *pb_fa* (°)	Bond effective modulus, *emod* (MPa)	Bond normal-to-shear stiffness ratio, *kratio*	Bond gap, *gap* (m)
Aggregate	0.6	100	1	0	0.02	35	5	2	0.0015
Geogrid	1	10	1	4.78	4.78	–	11.3	50	0.034
Subgrade	1	10	1	10	10	–	0.34	100	0.125

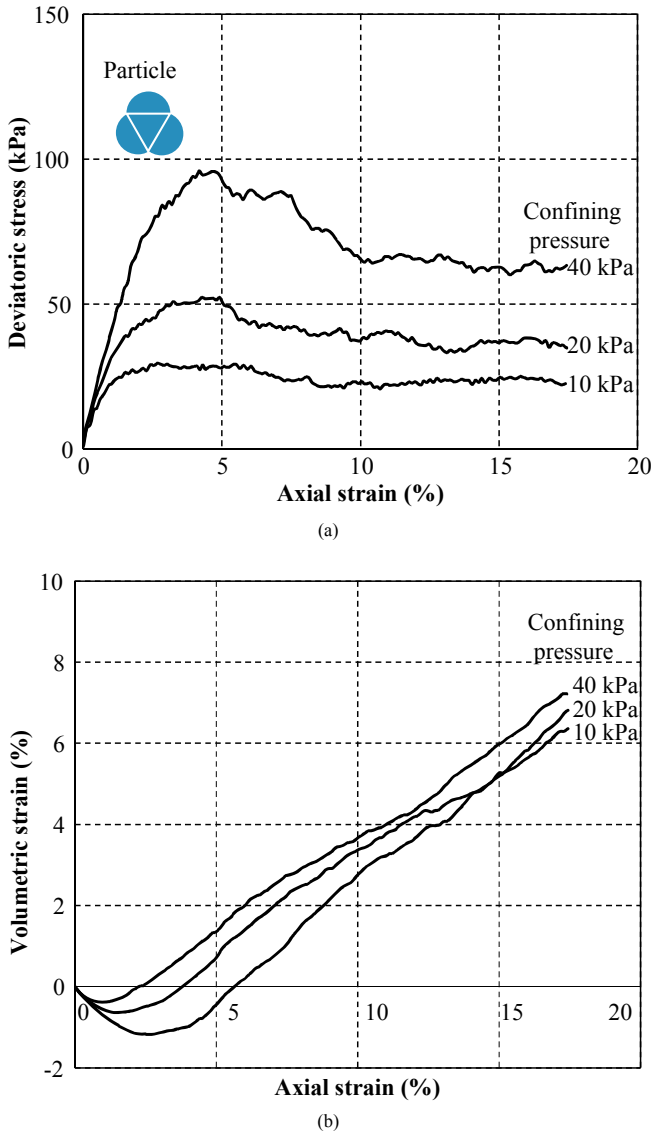

Fig. 2. Results from the biaxial test model.

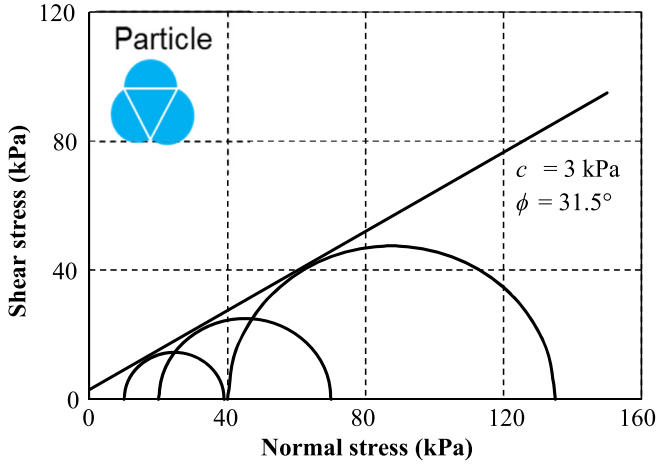

Fig. 3. Shear strength parameters measured from the biaxial test model.

2. Discrete element model and material parameters

DEM is a numerical method for simulating the behavior of discontinuous bodies such as granular soils. Unlike the more widely used finite element method (FEM) or finite difference method (FDM), DEM describes a numerical problem with bodies (balls, clumps, and walls) and contact models instead of numerical mesh and constitutive models. The behavior of each body (except for walls) follows the Newton's law of motion, and the interaction between two interacting bodies is described by the contact model.

The following subsections introduce the DEM compaction model and parameters used for the granular base course, the subgrade, and the geogrid. Since the objective is to qualitatively study the problem, parameters in the DEM model were calibrated to reflect the typical range of the material's behavior.

2.1. Granular base course

The granular base course material used in the DEM model was made of uniformly sized triangular particles. The triangular particles were used in this study instead of circular particles because angular particles can better simulate the interlocking effect between the geogrid and the base course material. In the PFC™ program, triangular particles can be created by bonding three balls in a triangular pattern to form a clump. The three balls in a clump are bonded rigidly to each other so that the clump cannot deform or break. The size of the triangular soil particles was set to have an equivalent-area diameter of 20 mm in all the cases analyzed in this study. The density of the aggregate particles was set as 2600 kg/m^3.

The contacts between the granular soil particles were modeled with the built-in linear parallel bond model in the PFC™ program. The linear parallel bond model is modified from the basic linear contact model by introducing a bond parallel to the direction of the contact surface. The linear parallel bond model can be used to simulate contacting bodies with a finite-sized cement-like material in between (similar to Fig. 1b), such as the fine content between coarse particles. The linear parallel bond contact model can transfer both force F_c and moment M_c between two contacted bodies:

$$F_c = F^l + F^d + \overline{F} \tag{1}$$

$$M_c = \overline{M} \tag{2}$$

In Eqs. (1) and (2), the linear force F^l and the dashpot force F^d are updated in the basic linear model, whereas the parallel bond force $\overline{F}$ and the parallel bond moment $\overline{M}$ are updated in the parallel bond model. The force-displacement and moment–torsion relationships are derived based on a material parameter called the effective bond

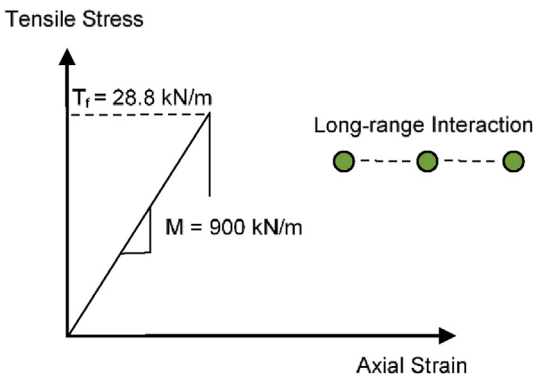

Fig. 4. The uniaxial tension behavior of the geogrid.

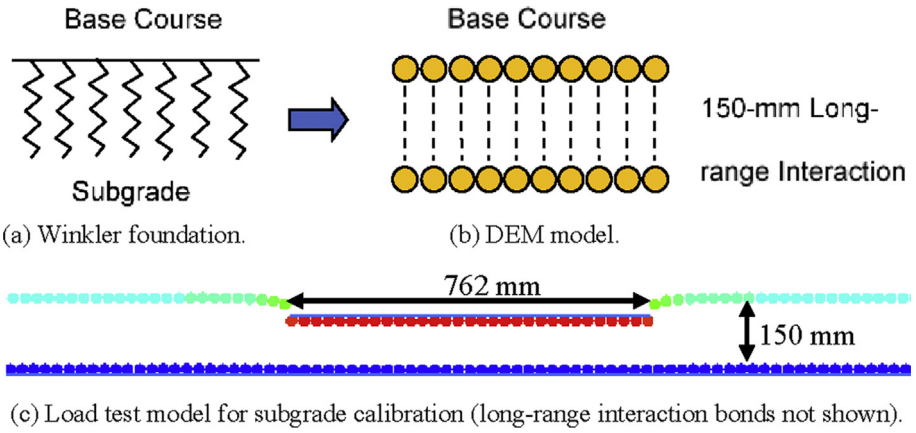

Fig. 5. Subgrade model with long-range interaction contacts.

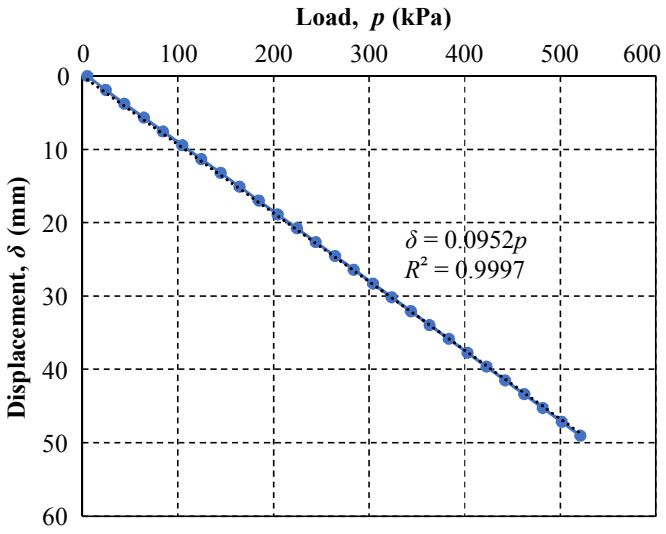

Fig. 6. Result of the modeled subgrade reaction modulus test.

modulus (*emod*) and the circular contact area with a radius proportional to the particle size (determined with a radius multiplier *pb_rmul*). The parallel bond can break based on a Mohr-Coulomb failure criterion with three parameters, the parallel bond cohesion (*pb_coh*), the parallel bond friction angle (*pb_fa*), and the parallel bond tensile strength (*pb_ten*). More details about the linear parallel bond model are provided in the software document of the PFC™ 5.0 (Itasca, 2017).

The body and contact parameters of the granular base material are listed in Table 1. It should be noted that many of the contact parameters in a DEM model cannot be physically measured from experiments. The parameter calibration in the DEM is usually done by simulating a physical material test such as the triaxial compression test for soil. In this study, body and contact model parameters for the granular base course layer were calibrated by modeling three biaxial compression tests (the 2D form of the triaxial compression test) at confining pressures of 10 kPa, 20 kPa and 40 kPa, respectively. The initial dimension of the biaxial test sample was 0.5 m wide and 1 m high. The initial porosity of the sample was set as 0.2. Theoretically, the result of the biaxial test is not affected by the sample size, therefore, a large test sample was

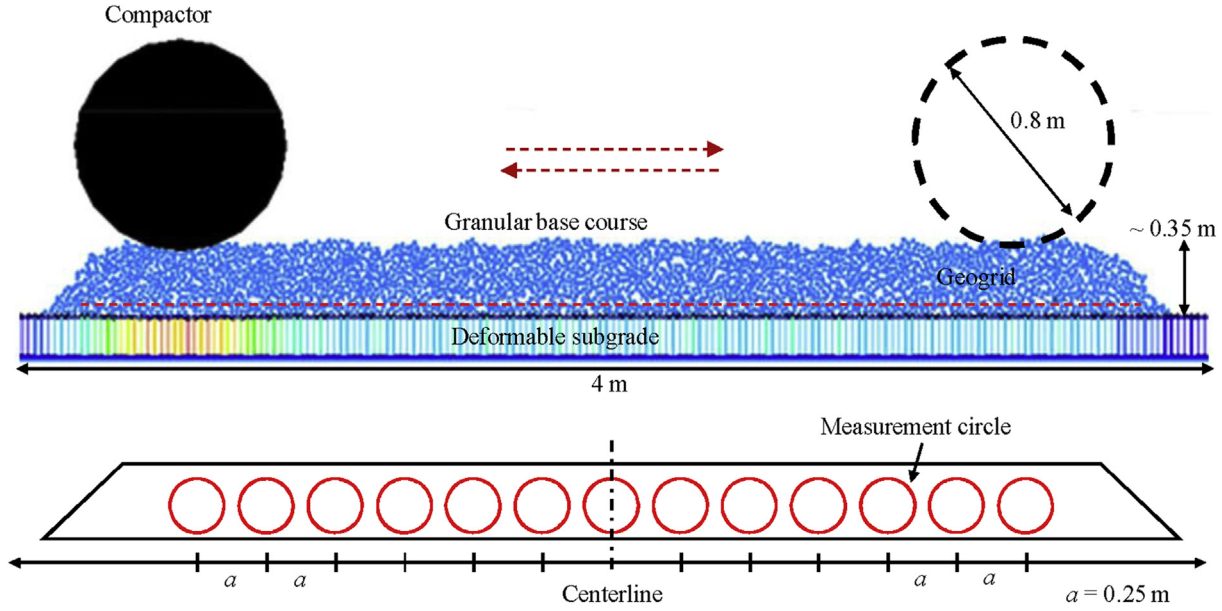

Fig. 7. Geometry of the compaction model.

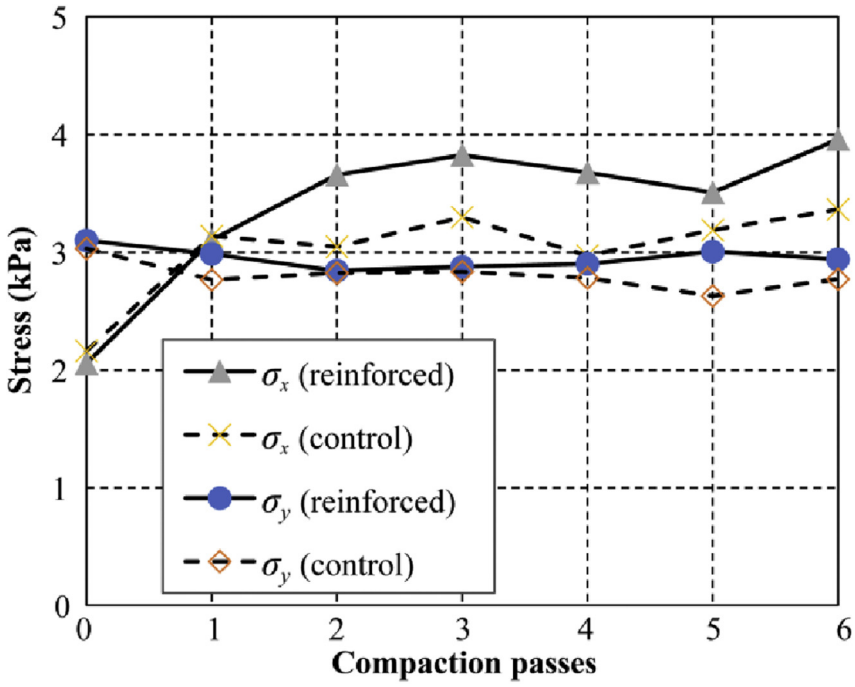

Fig. 8. Compaction-induced stress changing with the number of compaction passes.

used here to include more particles into the model and produce more reliable results. The initial dimension of the biaxial test sample was selected through multiple trials with gradually increased sample sizes. It was found that the 0.5 m × 1 m sample was able to produce smooth and repeatable stress–strain curves from the biaxial tests. Fig. 2 shows the results of the biaxial test model. Fig. 3 shows the Mohr circles and the shear strength parameters determined from the biaxial test model. With the body and contact parameters listed in Table 1, the granular soil showed a cohesion of 3 kPa and a friction angle of 31.5°. The small amount of cohesion was deliberately created in the calibration to simulate the effect of wet fine contents between the coarse particles in a typical base course material.

2.2. Geogrid

The geogrid was modeled with a series of equally spaced ball particles with a diameter of 3 mm and a center-to-center spacing of 40 mm. The ball particles interact with each other with a long-range interaction contact model which is newly introduced into the PFC™ 5.0. A long-range interaction contact model allows a particle to be linked to another particle in a specified distance range (or gap). The long-range interaction contact provides a more realistic way to simulate the interlocking between the geogrid and the granular soil. The contact model parameters (Table 1) are calibrated based on the Tensar BX 1200 geogrid product (in the cross-machine direction) with a tensile stiffness of 900 kN/m and an ultimate tensile strength of 28.8 kN/m (see Fig. 4).

In this study, the deformable subgrade soil was modeled with two parallel series of 20-mm diameter balls (see Fig. 5). The center-to-center spacing between the two layers of balls was 150 mm. Balls in the bottom layer were fixed in all directions, and balls in the top layer interact with those in the bottom layer by a long-range interaction contact model. Note that these two layers of balls do not simulate the real particles of the subgrade soil but provide a linear elastic foundation to the base course. The concept is similar to the Winkler foundation model (Fig. 5). One obvious advantage of this simplified approach is that it requires much few balls to simulate the subgrade soil. In addition, the subgrade stiffness can be easily calibrated by adjusting the bond effective modulus parameter in the contact model.

The contact model parameters (Table 1) for the soft subgrade were calibrated by modeling a plate load test. In this modeled load test, a 762-mm wide weightless load plate (modeled as a rigid wall) was placed on the top of a 4-m wide subgrade layer as described above. The load plate was set to move downward at a constant rate of 0.1 mm/s for a total displacement of 50 mm. Fig. 5c shows the deformed shape of the subgrade under the load plate. The relationship between the unbalanced pressure on the load plate and the displacement was recorded (as shown in Fig. 6). The result

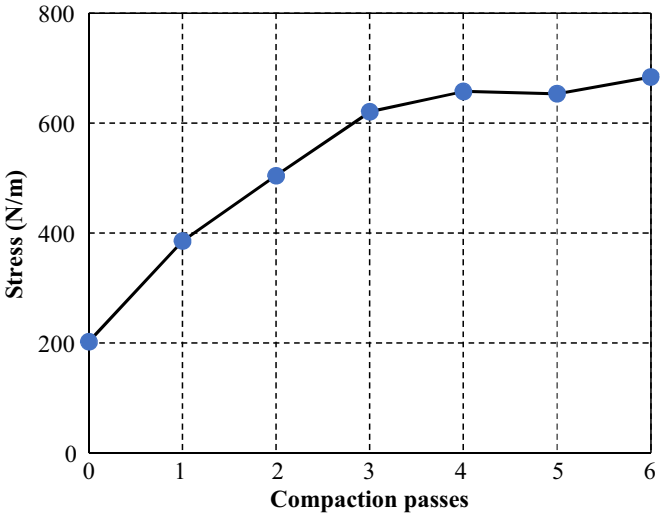

Fig. 9. Average residual tensile stress in the geogrid.

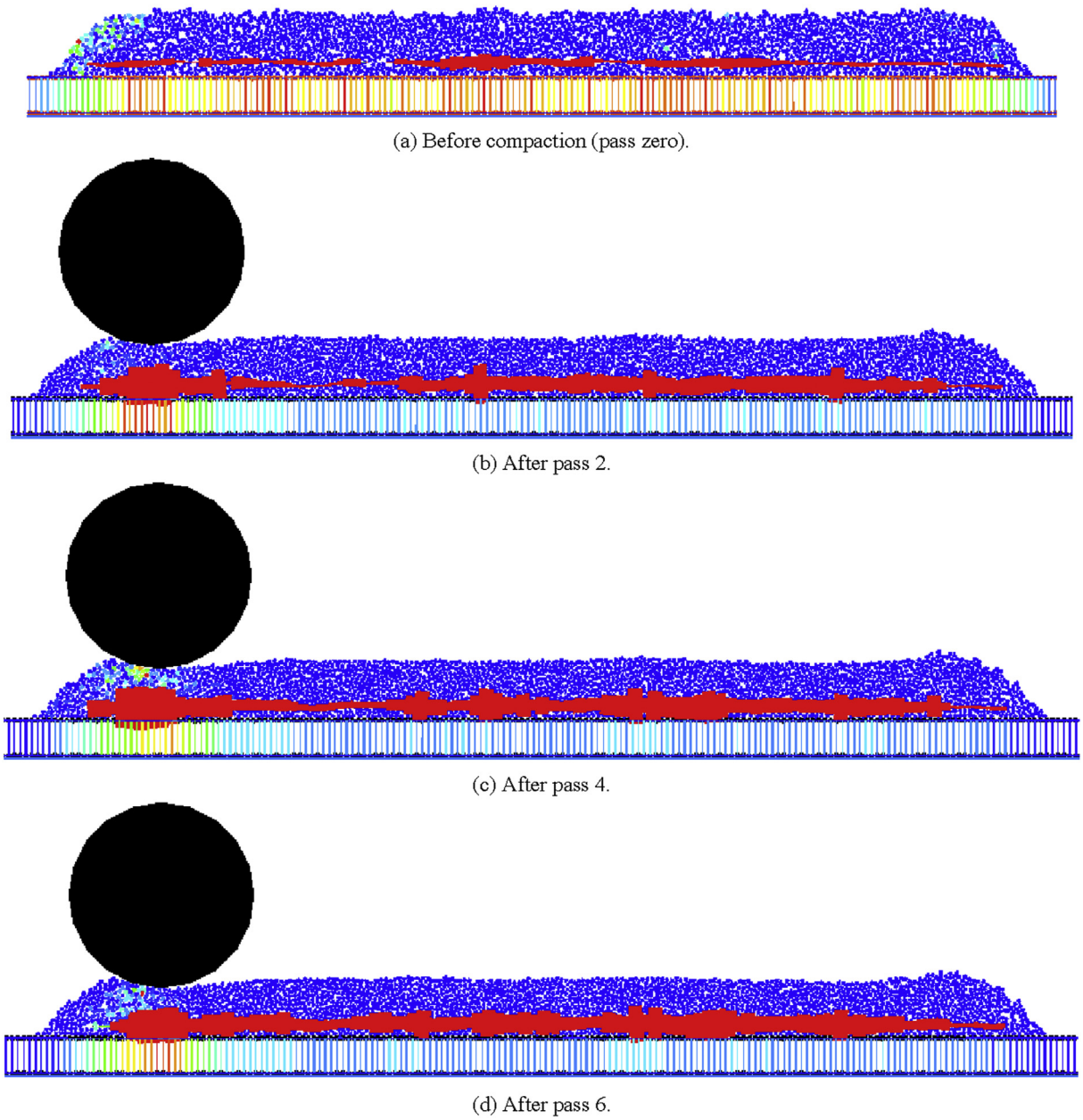

Fig. 10. Force chain of geogrid after each pass of compaction.

indicates that the subgrade modeled with the parameters in Table 1 showed a linear load–displacement response with a reaction modulus of $k = 10.5$ MPa/m.

3. DEM compaction model

3.1. Overview

The compaction model used in this study was a 4-m long and 0.35-m thick granular base course underlain by a deformable subgrade. The control case is an unreinforced granular base. In the case of the reinforced base course, a layer of geogrid was placed near the bottom of the granular base course. The roller compactor was modeled as a solid cylinder with a diameter of 0.8 m and a density of 1500 kg/m^3. Fig. 7 shows the geometry of the compaction model. For the compaction, the roller was set to spin at a rate 0.5 rad/s to produce a linear speed of about 0.2 m/s on the top of the aggregate layer. Six passes of roller compaction were simulated in the model, with back and forth as two passes. After each pass, the model was saved for further examination.

3.2. Generation of the base aggregate

The approach to generate the base aggregate affects its initial packing and stress condition. In practice, aggregates are dropped on the subgrade by dump trucks. To simulate the field situation, the subgrade layer was built first in the model. After that, 2500 triangular-shaped aggregate particles were generated at random locations and orientations in a rectangle area of 4 m wide and 0.7 m high from the subgrade surface. The aggregates were then allowed to drop freely by gravity to form a loose layer for compaction. In the reinforced case, a straight line of geogrid was created at a height of 0.09 m from the subgrade surface and then allowed to drop together with the aggregates. The total number of aggregate particles was

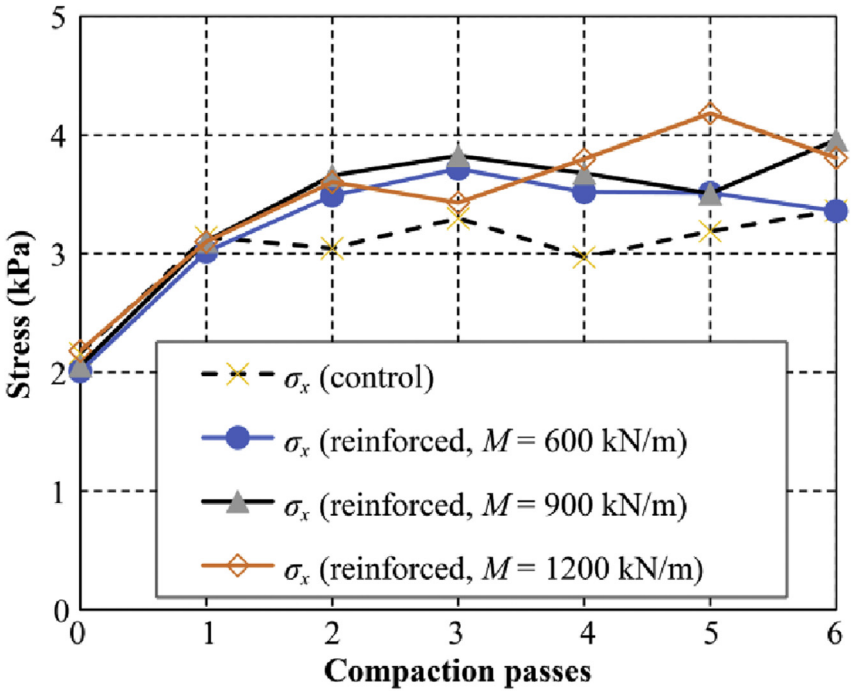

Fig. 11. Effect of geogrid stiffness on the compaction-induced stress.

determined by trial-and-error method so that a loose layer of about 300 mm was formed after the free drop. Finally, the roller compactor was placed on the surface of the aggregate and the system was solved for initial equilibrium before the compaction.

3.3. Earth pressure estimation

In this study, the stress condition of the granular base course was probed using the built-in "measure" function of the PFC™ 5.0 program. Stress is a continuum mechanics concept which cannot be easily defined in a discrete element model. The PFC™ 5.0 program provides a way to measure the average stress condition in a user-defined circular region. The average stress tensor, $\overline{\sigma}$, within the measurement circle can be calculated by the following equation (Itasca, 2017):

$$\overline{\sigma} = -\frac{1}{A^{\text{circle}}} \sum_{N^c} \overrightarrow{F}\overrightarrow{L} \tag{3}$$

where N^c is the total number of contacts within or on the boundary of the measurement circle, $\overrightarrow{F}$ is the contact force vector, $\overrightarrow{L}$ is the branch vector joining the centroids of the two bodies in contact, and A^{circle} is the area of the measurement circle.

It should be noted that the measure function (Eq. (1)) in PFC counts in all contact forces on all bodies (clumps and balls) within the measurement circle. This would include the long-range tensile force in the geogrid. Since we are only interested in the aggregate–aggregate and geogrid-aggregate contact forces, geogrid–geogrid contact forces have to be excluded from the stress measurement. This is achieved in the following steps. First, the state of the model at the end of each compaction pass is saved to a separate file. Second, remove all geogrid balls from the model. Finally, without solving the model, run the measurement function to determine the stress condition in the aggregate base.

In order to mitigate the inherent variation of the model and assess the representative stress condition of the granular base, 13 measurement circles were placed at 0, ±0.25 m, ±0.5 m, ±0.75 m, ±1 m, ±1.25 m and ±1.5 m from the centerline of the model. Each measurement circle has a diameter of 0.23 m. The locations of the 13 measurement circles are also shown in Fig. 7. After each pass of the roller compactor, the average values of the horizontal and vertical stresses at the 13 measurement circles were determined for further analysis.

4. Result and analysis

4.1. Effect of geogrid reinforcement

Fig. 8 shows the increase of compaction-induced stress in the soil with the number of compaction passes. The initial vertical stress σ_y and the horizontal stress σ_x in the control case and the geogrid-reinforced case were close to each other before the compaction (zero pass). After the first pass of compaction, both the reinforced and the control cases developed a significant amount of compaction-induced stress. At this moment, the horizontal stress in the soil exceeded the vertical stress. The compaction-induced stress continued to increase in the subsequent compaction passes. It is also evident that the reinforced case developed more compaction-induced stress than the control case.

Another way to assess the effect of geogrid in the compaction is by measuring the residual stress in the geogrid. In this study, the average residual stress in the geogrid was calculated by averaging all the long-range interaction contact forces between geogrid balls. Fig. 9 shows the change of average residual tensile stress in the geogrid with the number of compaction passes. It is shown that the residual stress in the geogrid also increases with the compaction passes. This result also demonstrates that the increased compaction-induced stress in a reinforced granular base is caused by the residual stress developed in the geogrid.

Fig. 10 presents the force chain of the long-range interaction contacts of the geogrid after different numbers of compaction passes. The thickness of the force chain represents the magnitude of the residual stress in the geogrid. The trend shown in Fig. 9 is

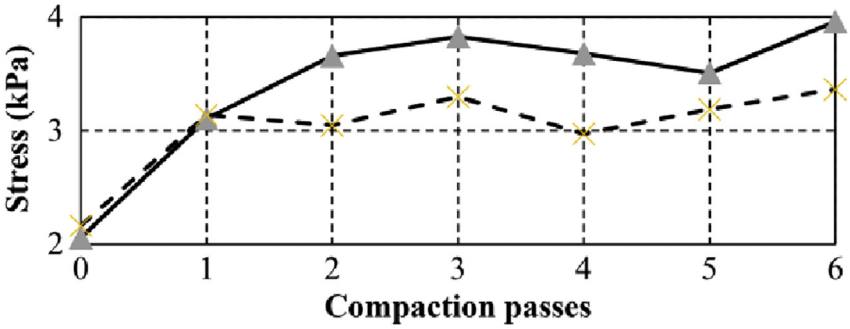

(a) Subgrade reaction modulus k = 10.5 MPa/m.

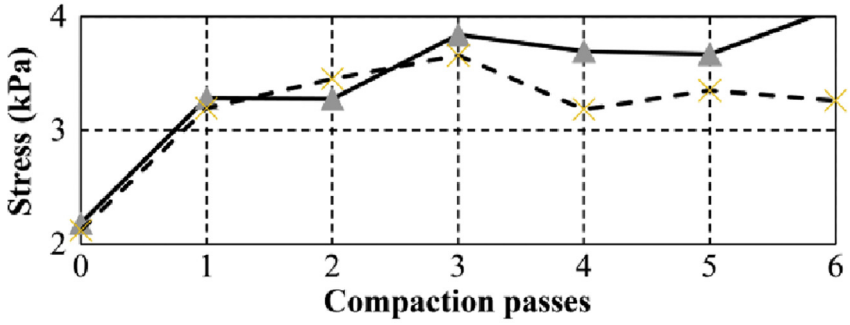

(b) Subgrade reaction modulus k = 5.3 MPa/m.

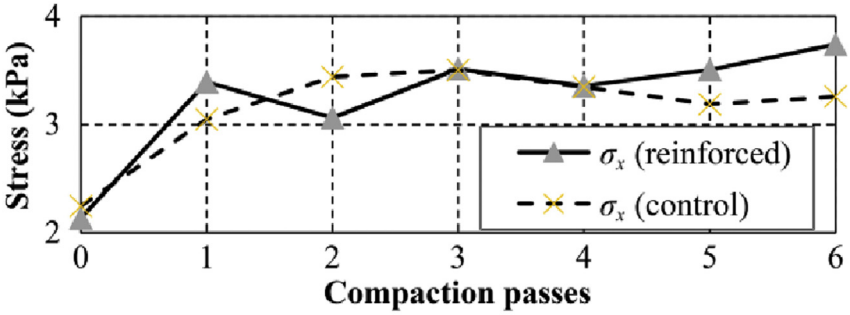

(c) Subgrade reaction modulus k = 2.6 MPa/m.

Fig. 12. Effect of subgrade modulus on the compaction-induced stress.

consistent with the change of compaction-induced stress in Fig. 8. Furthermore, subsequent compaction passes seem to improve the uniformity of the residual stress in the geogrid.

4.2. Effect of geogrid stiffness

A parametric analysis was performed to investigate the effect of the geogrid stiffness on the compaction-induced stress in the reinforced granualr base. Two additional cases were analyzed based on the baseline DEM model described previously with altered geogrid stiffness. The result in Fig. 11 shows a slight increase in the compaction-induced stress when the tensile stiffness of the geogrid increases from 600 kN/m to 1200 kN/m. However, the trend is not quite clear due to the variation of the curve. More cases need to be analyzed at a larger range of geogrid stiffness.

4.3. Effect of subgrade modulus

Another parametric analysis was performed to investigate the effect of the subgrade modulus on the compaction-induced stress in the reinforced granualr base. Two additional cases were analyzed based on the baseline DEM model described previously with different subgrade reaction moduli. Fig. 12 shows the horizontal earth pressures in the control and the reinforced cases when the subgrade reaction modulus was changed from 5.3 MPa/m to 10.5 MPa/m. After six passes of compaction, the amount of compaction-induced stress developed on different subgrades seemed to be similar. However, it is evident that more compaction passes are needed to mobilize the benefit of the geogrid reinforcement when the subgrade is relatively softer.

5. Conclusions and discussion

In this study, the effect of roller compactor on a poorly-graded granular base course underlain by a deformable subgrade, with and without geogrid reinforcement, was analyzed with a DEM model. The following conclusions can be drawn from this research:

(1) The long-range interaction contact provides a more realistic simulation of the soil-geogrid interaction in the 2D DEM

model. It also provides an efficient way to simulate a deformable subgrade.

(2) Geogrid reinforcement helps granular base courses to lock in additional compaction-induced stress during the roller compaction. The increased compaction-induced stress is caused by the confining effect from the residual tensile stress in the geogrid. The uniformity of the residual tensile stress in the geogrid improves with the number of compaction passes.

(3) Compaction induced-stress in the granular base courses seems to increase slightly with the tensile stiffness of the geogrid. However, this trend needs to be further confirmed by more analysis.

(4) The amount of compaction-induced stress developed in the granular base seems to be insensitive to the subgrade modulus. However, it is evident that more compaction passes are needed to mobilize the benefit of the geogrid reinforcement when the subgrade is relatively softer.

The development of compaction-induced stress in the reinforced granular base is a complicated process. This study represents a preliminary work and is limited to one type of base course material. Future work is needed to investigate the influences of gradation and other properties of the base course material. This study is also limited to one type of static roller compactor. Vibratory compactors and the effect of compaction energy need to be considered in future studies.

Conflict of interest

The authors wish to confirm that there are no known conflicts of interest associated with this publication and there has been no significant financial support for this work that could have influenced its outcome.

Acknowledgements

This research is supported by the Southern Plain Transportation Center (SPTC) under Award No. SPTC 15.1–06.

References

Chang G, Xu Q, Rutledge J, Horan B, Michael L, White D, Vennapusa P. Accelerated implementation of intelligent compaction technology for embankment subgrade soils, aggregate base, and asphalt pavement materials. Final report FHWA-IF-12–1002. Austin, USA: Transtec Group, Inc.; 2011.

Duncan JM, Seed RB. Compaction-induced earth pressures under K_0-condition. Journal of Geotechnical Engineering 1986;112(1):1–22.

Itasca. Software manual of PFC^{TM} 5.0 program. Minneapolis, USA: Itasca Consulting Group; 2017.

Kwon J, Tutumluer E, Al-Qadi IL. Validated mechanistic model for geogrid base reinforced flexible pavements. Journal of Transportation Engineering 2009; 135(12):915–26.

Kwon J, Tutumluer E. Geogrid base reinforcement with aggregate interlock and modeling of associated stiffness enhancement in mechanistic pavement analysis. Transportation Research Record Journal of the Transportation Research Board 2009;2116:85–95.

Perkins SW. Mechanistic-empirical modeling and design model development of geosynthetic reinforced flexible pavements. Final report FHWA/MT-01–002/99160-1A. Bozeman, USA: Montana State University; 2001.

Seed RB, Duncan JM. FE analyses: compaction-induced stresses and deformations. Journal of Geotechnical Engineering 1986;112(1):23–43.

Wu JTH, Pham TQ. An analytical model for evaluation of compaction-induced stresses in a reinforced soil mass. International Journal of Geotechnical Engineering 2010;4(4):565–72.

Yang X, Han J, Leshchinsky D, Parsons RL. A three-dimensional mechanistic-empirical model for geocell-reinforced unpaved roads. Acta Geotechnica 2013;8(2):201–13.

Te Pei is presently working as a PhD student in the Department of Civil and Environmental Engineering at Pennsylvania State University. He received his BSc degree from Oklahoma State University in 2017. His current research interest is discrete element modeling in studying the behavior of granular materials.

Dr. Xiaoming Yang is an assistant professor at the School of Civil and Environmental Engineering at Oklahoma State University in Stillwater, United States. He obtained his PhD degree in Civil Engineering from the University of Kansas in 2010. He also holds an MSs and a BSc Degree in Geological Engineering from Tongji University in Shanghai, China. Dr. Yang's research in recent years focuses on soil stabilization with geosynthetics, geotechnical information database, and pavement geotechnics.